DALTON
FULL PAPER

Monomer–polymer forms of solid, unsolvated, 5-coordinate halodimethyl(2-diphenylphosphinylethyl)stannanes, $XMe_2SnCH_2CH_2P(O)Ph_2$ (X = Cl, Br or I). Effects of different recrystallisation media

William T. A. Harrison,[a] R. Alan Howie,*[a] Craig M. Munro[a] and James L. Wardell[a,b]

[a] *Department of Chemistry, University of Aberdeen, Meston Walk, Old Aberdeen, Scotland, UK AB24 3UE. E-mail: r.a.howie@abdn.ac.uk*
[b] *Departamento de Química Inorgânica, Instituto de Química, Universidade Federal do Rio de Janeiro, CP 68563, 21945–970, Rio de Janeiro, RJ, Brazil*

Received 5th April 2001, Accepted 10th July 2001
First published as an Advance Article on the web 17th August 2001

As determined by X-ray crystallography, unsolvated $XMe_2SnCH_2CH_2P(O)Ph_2$ (X = Cl, Br or I) crystallises in two forms: linear chain polymers, obtained by recrystallisation from EtOH or MeOH, and chelated monomers from non-hydroxylic solvents, such as chlorocarbons and acetone. The linear chains are formed by intermolecular Sn–O interactions [at 301 K, 2.339(2) (X = Cl): 2.309(3) (X = Br): 2.282(3) Å (X = I)]: the resulting 5-coordinate tin centres have trigonal bipyramidal geometries, with the halide and the oxygen atoms in axial sites. The chelated forms, with intramolecular Sn–O interactions [also at 301 K: 2.3989(15) (X = Cl): 2.381(2) (X = Br): 2.386(2) Å (X = I)], also contain 5-coordinate tin centres, with trigonal bipyramidal geometries and with the halide and the oxygen atoms in axial sites. As shown by X-ray powder patterns, cooling the melt of *polymer*-(**2**: X = I) gave *chelate*-(**2**: X = I). The isothiocyanato analogue, $(SCN)Me_2SnCH_2CH_2P(O)Ph_2$, crystallises in the monomeric chelated form from all solvents attempted for recrystallisation [Sn–O = 2.3865(19) and 2.3920(19) Å], in two independent molecules.

Introduction

Structural studies of halotriorganostannanes, R_3SnX, in which at least one of the organic groups bears a donor substituent, have revealed a strong tendency to form five-coordinated species as a consequence of donor group–tin coordination.[1] For compounds with suitably sited donor groups, intramolecular complexation can create chelate rings. As illustrated with oxygen-containing donor groups, the most frequently reported chelate ring is five membered[2–4] with four membered[5] and six membered chelate rings[6] also known. If the geometry prevents chelation, or when the chelate ring would be greater than six membered, or for other reasons, intermolecular complexation occurs instead (Fig. 1). As shown with $HO(CH_2)_nSnCl_3$[7] and $MeC(O)O(CH_2)_nSnCl_3$,[8] the potential chelate size is most important: chelates are formed when n = 3 or 4, but not when n = 5; instead intermolecular associations occur.

Due to the chelate effect,[9] it is to be expected that if five-membered chelates can be formed, donor–tin interactions will be intramolecular; as reported, for example, for $XMe_2SnCH_2CH_2P(O)PhBu^t$, (**1**: X = Br),[4a] and for $XMe_2SnCH_2CH_2P(O)Ph_2$ (**2**: X = F),[4b] both recrystallised from CH_2Cl_2/hexane. However, a study of the related compounds, (**2**: X = Cl, Br or I), has indicated a more complex situation. As shown by X-ray crystallography, the expected chelated molecular complexes of **2**, *chelate*-(**2**: X = Cl, Br or I), are obtained on recrystallisation from non-hydroxylic solvents (*e.g.* Me_2CO, $CHCl_3$ and CH_2Cl_2), but when recrystallised from alcohols, such as MeOH or EtOH, they have polymeric structures, *polymeric*-(**2**: X = Cl, Br or I), in which molecules are linked into chains by Sn–O intermolecular coordination. The isothiocyanato compound, (**2**: X = NCS), however, crystallises in the chelate form from all solvents tried. The tin centres in both sets of unsolvated complexes are 5-coordinated, with trigonal bipyramidal geometries and with the halide and the oxygen ligands in the axial sites.

At the outset of the study presented here, we did not anticipate the occurrence of two different crystalline forms for these compounds. Indeed, the crystal structure of a sample of (**2**: X = I), recrystallised from EtOH, at 150 K was only carried out as an undergraduate exercise, on the assumption that it would have a similar chelated structure to those reported for (**1**: X = Br) and (**2**: X = F) at room temperature.[4] The subsequent result and the need to establish whether the structural differences resulted from the change of compound, halide, temperature or the recrystallisation medium, led to the study now reported.

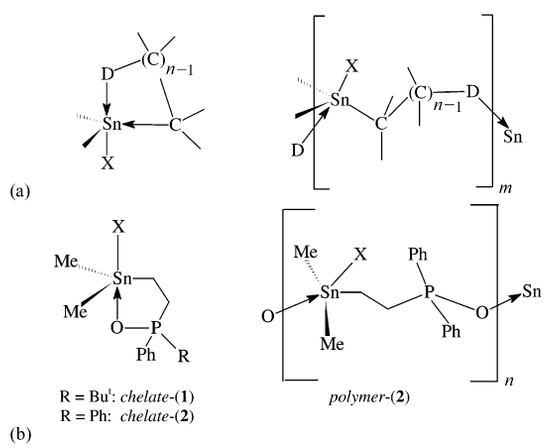

Fig. 1 (a) General representations of intramolecular and intermolecular coordination in R_3SnX compounds: (b) chelate and linear chain forms of **1** and **2**.

Results and discussion

General aspects

Compounds (**2**: X = Cl, Br or I) have been previously obtained from $Me_3SnCH_2CH_2PPh_2$.[10] For example, (**2**: X = Br or I) have

been prepared from the reaction of $Me_3SnCH_2CH_2PPh_2$ with Br_2 or I_2 in MeOH solution.[10b] Synthesis of (**2**: X = Br, I or NCS) in this study was generally achieved by an exchange reaction in acetone solution between NaX and (**2**: X = Cl): (**2**: X = Cl) was prepared from (**2**: X = Me) and HCl in ether solution by a similar procedure used to obtain (**1**: X = Cl).[4] NMR spectral data (Table 1) and X-ray crystallography showed that fully exchanged products could be obtained by the exchange route. Compound (**2**: X = I) was also prepared from (**2**: X = Me) and I_2 in $CHCl_3$.

Solution behaviour of **2** and related compounds has been extensively explored in chloroform solutions.[10] NMR and IR spectral data suggest that (**1**: X = Cl or Br)[4] and (**2**: X = Cl, Br or I)[10] are 5-coordinate in chlorocarbon solutions at ambient temperature, *e.g.*, ν(PO) = 1140–1130 cm^{-1} in **1** and **2**, compared to values of *ca.* 1185 cm^{-1} in four-coordinate $Me_3SnCH_2CH_2P(O)PhR$ (R = Bu^t or Ph). The similar NMR parameters for (**2**: X = Cl or Br) in CD_3OD and $CDCl_3$ solutions, as shown in Table 1, indicate that 5-coordinate species must also occur in CD_3OD solutions. Solution NMR spectroscopy is however considered insufficiently sensitive to distinguish between the monomer and polymer forms of **2**,

Table 1 NMR spectral details, [δ(ppm), J(Hz)] for $XMe_2SnCH_2CH_2P(O)Ph_2$ in $CDCl_3$ and CD_3OD

	^{1}H NMR				^{119}Sn NMR
X	δ(MeSn) [J(Sn–H)]	δ($SnCH_2$) J(H–H) [J(Sn–H)] {J(P–H)}	δ(CH_2P) J(H–H) [J(Sn–H)] {J(P–H)}	δ(Ph)	δ^{119}Sn [J(Sn–P)]
SCN	0.57 [71.6/68.6]	1.36 7.5 [72.8, 69.6] {19.8}	2.59 7.5 [106.8, 102.4] {9.2}	7.46–7.60	−49.3 [nr]
Cl	0.72 [69.4/66.7]	1.45 7.5 [*ca.* 70] {20.2}	2.61 7.5 [108, 104] {8.9}	7.42–7.62	10.8; 11.0[a] [43.9]
Cl [in CD_3OD]	0.62 [70.0/66.3]	1.37 7.9 [nd] {18.1}	2.80 7.9 [nd] {9.6}	7.51–7.73	*ca.* 16 [nd]
Br	0.83 [69.1/66.0]	1.55 7.5 [69.1, 66.3] {19.8}	2.61 7.5 [107.4, 102.6] {9.2}	7.45–7.63	−1.7; 1.7[a] [42.7]
Br [in CD_3OD]	0.66 [68.7/66.0]	1.45 7.5 [67.2, 64.8] {18.5}	2.89 7.5 [*ca.* 105, 101] {8.9}	7.54–7.75	—
I	1.00 [68.1/65.3]	1.68 7.5 [67.7, 65.0] {20.1}	2.60 7.5 [107.4, 102.6] {8.9}	7.47–7.63	−31.8; −31.1[a] [41.3]
I [in CD_3OD]	0.71 [68.1/65.2]	1.50 7.5 [67.7, 65.0] {18.5}	2.92 7.5 [*ca.* 105, 101] {9.3}	7.55–7.75	nd
Me[a]	0.04 [53.5]	0.90 nr	2.30 nr	7.38–7.75	11.4
Me [in CD_3OD]	0.09 [54.0]	0.85	2.44	7.48–7.69	nd

	^{13}C NMR				
X	δ(MeSn) [J(Sn–C)] {J(P–C)}	δ(α-C) [J(Sn–C)] {J(P–C)}	δ(β-C) [J(Sn–C)] {J(P–C)}	δ(Ph) {J(P–C)}	Other
SCN	0.1 [*ca.* 530] {2.3}	8.7 [520] {3.8}	25.5 [*ca.* 18] {67.7}	130.3 {12.1}, 130.5 {103}, 131.5 {9.9},134.2 {3.1}	138.2 (SCN)
Cl	3.1 [500/481] {3.1}	11.6 [495] {4.6}	26.1 [19] {68.0}	130.2 {12.2}, 130.7 {100}, 131.7 {9.9}, 134.0 {3.1}	46.4[δ^{31}P][a]
Cl [in CD_3OD]	0.7 [*ca.* 500] {nd}	11.0 [nd] {nd}	24.8 [nd] {66.6}	130.0 {12.2}, 130.6 {100}, 131.6 {10.6}, 133.8 {3}	nd
Br	4.1 [nd] {2.3}	12.7 [nd] {3.8}	26.3 [nd] {68.4}	130.3 {12.2}, 130.5 {100}, 131.7 {9.9}, 134.1 {2.3}	45.4[δ^{31}P][a] 43.4[δ^{31}P][a]
I	5.4 [*ca.* 490] {2.3}	14.1 [*ca.* 490] {4.6}	26.4 [nd] {68.4}	130.3 {12.1}, 130.6 {96}, 131.7 {9.8}, 134.1 {3.1}	45.9[δ^{31}P] 44.4[δ^{31}P][a]

[a] From ref. 10(*a*); nr not reported; nd not determined.

Table 2 Melting points and heating–melting behaviour of **2**

Compound	Recryst. solvent	mp/°C (Kofler hot stage)	DSC/°C [J g^{-1}] Initial heat stage	DSC/°C [J g^{-1}] Reheat stage, after heating to 300 °C, and cool stage
(**2**: X = Cl)	Me_2CO	126–130	128–130 [−74.3], 154–155 [−1.4]	229–230 [−6.7], 232–234
	EtOH	129–131	128–130 [−48.2]	229–230 [−3.2] 232–233 [−1.2]
(**2**: X = Br)	CH_2Cl_2/C_6H_{12}	[140–141][a]	—	—
	CH_2Cl_2		141–146 [−74.0], 187–190 [−23.3]	228–230 [−8.5], 232–234
	Me_2CO	138–140	139–142 [−77.2], 165–166 [−1.7]	—
	EtOH	192–194	188–193 [−81.3]	229–230 [−3.7]
(**2**: X = I)	CH_2Cl_2	144–146		
	$CHCl_3$	146–148	145–148, 209–211	
	Me_2CO	208–9	145–146 [−1.9], 146–148 [3.1], 209–210 [−89.0]	229–230 [−7.7], 232–234
	MeOH	208–211	—	—
	EtOH	218–222	208–212 [−91.8]	229–230 [−6.7], 232–234
(**2**: X = NCS)	CH_2Cl_2	118–120		
	MeOH	117–119	116–118 [−54.4]	No peaks

DSC: heating at 10 °C per minute to 300 °C. [a] Ref 10.

since both types of structure contain the same bonding atoms to tin and basically the same geometry at tin. The very slight differences in δ^1H values [*i.e.* downfield shifts for the Me–Sn and Sn–CH_2 protons, and the upfield shifts for CH_2–P and P–Ph protons, on changing the solvent from CD_3OD to $CDCl_3$] could arise from the slight changes between the polymer/monomer forms or equally from the solvent change. As 4-coordinate (**2**: X = Me) also exhibits similar changes in δ^1H values for the Sn–CH_2CH_2 protons, on solvent change from $CDCl_3$[10] to CD_3OD, solvent effects cannot be ignored. The very similar environments about tin in the chelate and polymeric forms of **2** would result in very similar δ^{119}Sn values, as is found: the difference in δ^{119}Sn values for (**2**: X = Cl) [$\Delta\delta^{119}$Sn ≈ 5 ppm, between CD_3OD and $CHCl_3$ solutions] is almost negligible considering the large ppm range for organotin compounds as a whole.

Behaviour on heating

As indicated in the Introduction, the solvent used for recrystallisation of (**2**: X = Cl, Br or I) influenced the solid state structures. Table 2 lists the melting points measured on a Kofler hot stage and the thermal behaviour studied by DSC and TGA/MS for compounds **2**, recrystallised from different solvents. In the DSC experiments, the heating rate was maintained at 10 °C min^{-1}: a similar heating rate was aimed for in the Kofler hot stage determinations of melting points. Some differences in the melting points were obtained for samples even recrystallised from the same solvent. One variable appeared to be the rate at which recrystallisation was performed: furthermore, samples obtained from solution (of analytically pure materials) left to completely evaporate had wider ranging melting points. The results reported in Table 2 were for the initial crystals obtained from solutions on slight evaporation of the solvent. In all cases, the compounds were stable up to their melting points, onset of decomposition being 226–230, 228–232, 218–225 and >250 °C for X = Cl, Br, I and NCS, respectively. Decomposition of (**2**: X = I), studied by TGA/MS, began just after melting: by 290 °C, the weight loss was 26% with *m/z* fragments of 28, 44, 125, 140, 154 and 165 observed. As shown in the reheat cycles of the DSC runs, heating (**2**: X = Cl, Br or I) to 300 °C led to complete loss of the starting compound. In all cases, the reheat cycle showed a melt at *ca.* 230–235 °C: however, the J g^{-1} values [−1.2 to −8.5], based on the amount of material used initially, suggested that only a small amount of a new fusible material was present [*cf.* values determined for the initial melting of **2** were generally in the region 70–90 J g^{-1}].

No polymer–monomer transitions were indicated in the DSC of samples taken to below their melting points. However, evidence was gained for such a transition from a melt. A sample of *polymeric*-(**2**: X = I), heated to melting at 215 °C and then cooled to 20 °C, yielded as product a material whose X-ray powder pattern proved to be identical to that calculated for the chelate form, *chelate*-(**2**: X = I). Calculated powder diffraction patterns are shown for *chelate*- and *polymeric*-(**2**: X = I) in Fig. 2. Another sample of *polymeric*-(**2**: X = I), similarly heated just to its melting point, followed by cooling to room temperature, indicated a crystallisation peak at 75 °C [32.5 J g^{-1}] and a fairly large melting range from 134 to 139 °C [−36.8 J g^{-1}] on reheating. The fact that the chelate-form is formed from the melt indicates that this is the more stable form.

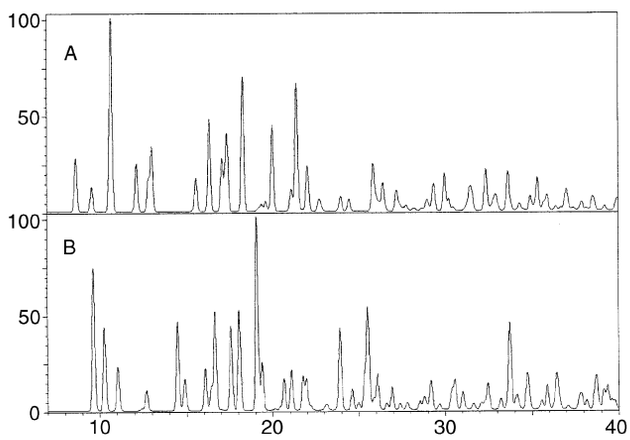

Fig. 2 Theoretical powder diffraction patterns for (a) *chelate*- and (b) *polymeric*-(**2**: X = I) calculated from the results of single crystal structure analysis. Relative intensity (*y*-axis) is plotted against 2θ for Cu-Kα_1 (*x*-axis, λ = 1.54056 Å).

Polymeric-(**2**: X = Cl), mp 127–128 °C, when heated to 170 °C, *i.e.* well below its decomposition point, followed by cooling, gave no exothermic or endothermic peaks on reheating from ambient to 170 °C: a glass or an amorphous product was indicated, however, no glass transition temperature was detected. Similarly no peaks, either exothermic or endothermic, were observed in the reheat stage of the DSC run for *chelate*-(**2**: X = SCN), previously heated to 250 °C.

Solid state structures of 2

Crystal structures of *chelate*-(**2**: X = Cl, Br, I and NCS) and *polymeric*-(**2**: X = Cl, Br and I) were determined. The crystals used in the X-ray structure determinations were obtained as the first crop from solutions by slow evaporation of the solvents at ambient temperature (301 K). The numbering schemes and molecular arrangements for *chelate*-(**2**: X = Cl, Br and I), *chelate*-(**2**: X = NCS) and *polymeric*-(**2**: X = Cl, Br and I) are shown in Fig. 3–5, respectively: the actual compounds illustrated in Fig. 3 and 5 are bromides. No structural change occurs for *chelate*-(**2**: X = I) between 150 and 301 K: as expected the unit cell volume is slightly reduced, by 2.5%, at the lower

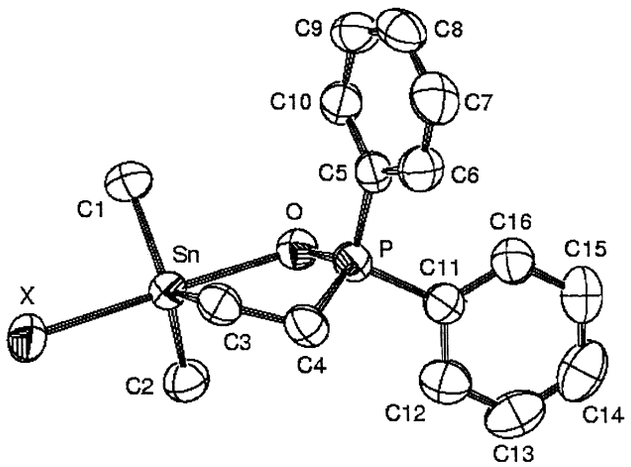

Fig. 3 The molecule and atom labelling scheme for *chelate*-(**2**: X = Cl, Br and I). The molecule illustrated is that of X = Br with non-H atoms shown as 50% ellipsoids and H atoms omitted for clarity.

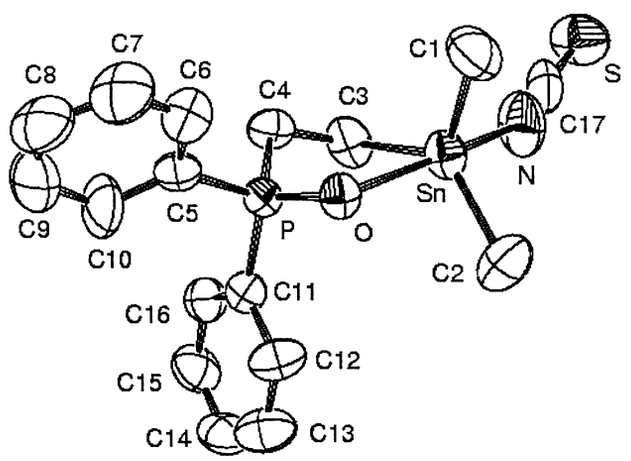

Fig. 4 Molecule A of *chelate*-(**2**: X = SCN) with suffixes A omitted. Molecule B is very similar and apart from the suffixes labelled in an identical manner. The representation is otherwise the same as in Fig. 3 and 5.

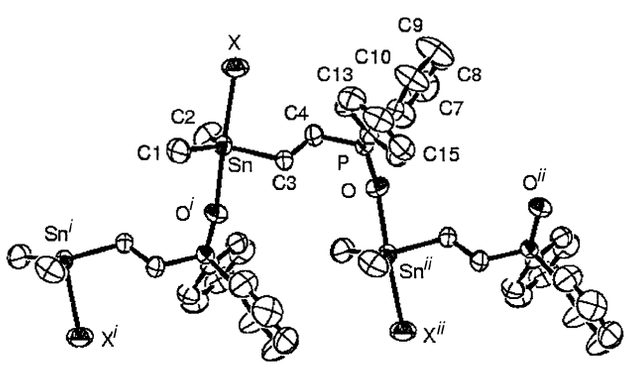

Fig. 5 A portion of a chain of molecules of *polymeric*-(**2**: X = Cl, Br and I). The numbering scheme and mode of representation are the same as in Fig. 3. The example shown is X = Br. Selected atoms are labelled. Symmetry operations *i*: $x + 1/2, -y + 1/2, -z$; *ii*: $x - 1/2, -y + 1/2, -z$.

temperature. The structures of *polymeric*-(**2**: X = Cl, Br and I) are isostructural. The molecular structures of the four chelates, *chelate*-(**2**: X = Cl, Br, I and NCS), are similar, but only *chelate*-(**2**: X = Cl and Br) are isostructural.

Tables 3 and 4 list selected bond lengths and angles for *chelate*-(**2**: X = Cl, Br, I and NCS), and *polymeric*-(**2**: X = Cl, Br and I), respectively. Both sets of structures have trigonal bipyramidal geometries, with the oxygen and halide or pseudo-halide atoms in axial positions. The greater distortions from ideal trigonal bipyramidal geometries are experienced by the chelated complexes, for example, the *trans*-axial angles, X–Sn–O, range from 169.41(11) to 173.24(4)° in *chelate*-(**2**) and from 175.92(8) to 176.30(8)° in *polymeric*-(**2**). Much of this distortion arises from the small chelate bite angles [79.63(7) to 81.63(9)°] in *chelate*-(**2**). The chelate rings in *chelate*-(**2**) have near envelope conformations with flaps at C4.

The O–Sn bond lengths in *polymeric*-(**2**) decrease in the sequence Cl [2.339(2)] > Br [2.309(3)] > I [2.282(3) Å]: this suggests that the acceptor strengths of the tin centres in the polymeric complexes increase in the sequence (**2**: X = I) < (**2**: X = Br) < (**2**: X = Cl). Of interest, the Sn–O bond lengths in *chelate*-(**2**), including those for the isothiocyanato compound, fall into a much smaller range of values, from 2.373(4) to 2.3989(15) Å, with all being larger than the values in *polymeric*-(**2**). The closeness of the values in *chelate*-(**2**) do not allow any distinction to be made between the Lewis acidities of the tin centres. The larger Sn–O distances and the relative inability to distinguish the acceptor strength sequence in the chelated forms are considered to be due to steric factors having a far more significant influence on the ligand positions about tin in the chelated form than in the linear chain, polymeric, form.

It is also noticeable that the P–O bond lengths in *polymeric*-(**2**) are shorter than those in *chelate*-(**2**). Comparison of the Sn–O and Sn–X bond lengths in the *chelate*-(**2**)/*polymeric*-(**2**) pairs clearly shows that shorter Sn–O bonds result in longer Sn–X bonds. While the differences in each of the Sn–O and Sn–I bond lengths in *chelate*-(**2**: X = I) at 150 and 301 K are scarcely significant, they are in the sense expected for stronger Sn–O complexation at the lower temperature.

Comparison of the structures of (**1**: X = Br) and *chelate*-(**2**: X = Br) indicates that the stronger Sn–O interaction occurs with the former compound. In (**1**: X = Br), the Sn–O and Sn–Br bond lengths are 2.324(6) and 2.684(1) Å, while in *chelate*-(**2**: X = Br), the equivalent bonds have lengths of 2.381(2) and 2.6803(4) Å, respectively. While steric factors will be of importance in (**1**: X = Br) and will affect bond lengths, the trend is in the direction suggested by the relative inductive affects of the Bu^t and Ph groups.

The Sn–O bond lengths found [3] for the 5-membered chelates, 1-(XMe_2Sn)-2-(MeO_2C)-1,4-cyclohexadienes were 2.469(3) (X = Cl), 2.468(7) (X = Br) and 2.391(5) Å (X = I): all are slightly longer than the corresponding values determined for the same X ligand in *chelate*-(**2**).

IR spectra of solid 2

The solution ν(P=O) values (in CCl_4) for (**1**: X = Cl), (**2**: X = Br) [chelate], (**2**: X = I) [chelate] and (**2**: X = Me), were earlier reported to be 1138, 1157, 1154 and 1198 cm^{-1}, respectively. The most intense band in the 1200–1100 cm^{-1} region for solid (**2**: X = Me) in a KBr disc is at 1181 cm^{-1}, with a less intense band at 1120 cm^{-1}. Phosphine oxide–tin coordination in solid (**2**: X = halide or NCS) is indicated by the bathochromic shifts of the P=O stretching frequency. The monomeric species and the linear chains exhibit distinct bands in ν(P=O), see Table 5. For *chelate*-(**2**: X = Cl and NCS), the most intense band is at 1139–1133 cm^{-1}, with shoulders at 1158–1156 cm^{-1}, while for *chelate*-(**2**: X = I), there is a single broad band with a maximum at 1133 cm^{-1}. For *polymeric*-(**2**: X = Cl and Br), the major band is *ca.* 1167 cm^{-1} with a shoulder at 1159 cm^{-1}, while for *polymeric*-(**2**: X = I) the situation is reversed in that the main band is at 1156 cm^{-1} and the shoulder is at 1162 cm^{-1}. All the linear chain forms exhibit an additional strong band at 1126 cm^{-1}. The differences in the ν(P=O) bands for the two classes of structures are useful diagnostically. Spectral differences are also found between the chelates and the linear chains in the region 600–150 cm^{-1}. For the monomeric complexes, peaks are generally found in the ranges 565–559, 536–530, 445–442 and 388–382 cm^{-1}; while for the linear chains, peaks are generally

Table 3 Bond lengths (Å) and angles (°) for monomeric chelated **2**

	(**2**: X = Cl) 301 K	(**2**: X = Br) 301 K	(**2**: X = I) 301 K	(**2**: X = I) 150 K	(**2**: X=SCN) 301 K molecule 1	(**2**: X = SCN) 301 K molecule 2
Sn1–C1	2.123(3)	2.127(3)	2.121(5)	2.110(8)	2.120(4)	2.100(4)
Sn1–C2	2.117(2)	2.114(3)	2.116(5)	2.129(7)	2.113(4)	2.117(4)
Sn1–C3	2.156(2)	2.156(3)	2.160(4)	2.154(7)	2.146(3)	2.144(3)
Sn1–O1	2.3989(15)	2.381(2)	2.386(2)	2.373(4)	2.3865(19)	2.3920(19)
Sn1–X	2.5114(7)	2.6803(4)	2.9363(4)	2.9399(7)	2.205(3)	2.211(3)
P1–O1	1.5107(16)	1.513(2)	1.519(3)	1.518(5)	1.5101(19)	1.510(2)
C3–C4	1.523(3)	1.536(4)	1.518(6)	1.534(9)	1.534(4)	1.521(4)
C4–P1	1.806(2)	1.801(3)	1.803(4)	1.794(7)	1.797(3)	1.794(3)
C2–Sn1–C1	116.73(11)	117.03(15)	116.6(2)	117.4(3)	117.33(18)	116.7(2)
C2–Sn1–C3	117.30(10)	117.86(13)	119.0(2)	117.9(3)	125.28(16)	118.74(18)
C1–Sn1–C3	123.18(10)	122.87(14)	122.9(2)	123.4(3)	116.42(16)	123.80(15)
C2–Sn1–O1	86.62(9)	87.25(12)	89.54(16)	90.1(2)	87.79(13)	89.56(14)
C1–Sn1–O1	87.25(9)	87.96(11)	87.56(16)	87.8(2)	91.68(13)	90.30(11)
C3–Sn1–O1	79.63(7)	80.02(10)	81.00(12)	81.1(2)	81.12(9)	81.63(9)
C2–Sn1–X	97.10(8)	96.82(10)	97.84(15)	97.6(2)	96.06(16)	94.61(17)
C1–Sn1–X	96.04(8)	95.19(10)	94.87(15)	94.5(2)	95.26(17)	94.38(14)
C3–Sn1–X	93.63(7)	93.04(9)	89.71(11)	89.35(19)	88.63(13)	89.91(13)
O1–Sn1–X	173.24(4)	173.01(5)	170.16(6)	169.83(11)	169.41(11)	171.54(11)
O1–P1–C4	108.07(10)	108.21(13)	107.45(16)	107.5(3)	107.14(12)	107.76(12)
P1–C4–C3	108.90(16)	108.4(2)	108.3(3)	107.7(5)	108.3(2)	110.5(2)
C4–C3–Sn1	112.69(16)	112.4(2)	113.3(3)	113.0(5)	112.89(19)	114.43(19)
O1–Sn1–C3–C4	−31.55(17)	−31.1(2)	24.1(3)	24.3(5)	24.1(2)	17.7(2)
Sn1–C3–C4–P1	46.9(2)	46.7(3)	−44.0(3)	−44.5(7)	−44.4(3)	−36.8(3)
C3–C4–P1–O1	−38.1(2)	−38.8(3)	45.8(3)	46.5(6)	46.3(2)	42.1(2)
C4–P1–O1–Sn1	13.12(14)	14.35(18)	−26.0(2)	−26.8(4)	−26.44(15)	−26.95(15)
P1–O1–Sn1–C3	7.84(11)	6.99(14)	4.24(18)	4.4(3)	4.32(13)	8.08(13)

Table 4 Bond lengths (Å) and angles (°) for polymeric **2**

	(**2**: X = Cl) 301 K	(**2**: X = Br) 301 K	(**2**: X = I) 301 K
Sn1–C1	2.121(3)	2.121(4)	2.129(4)
Sn1–C2	2.119(3)	2.119(4)	2.112(4)
Sn1–C3	2.140(3)	2.147(4)	2.141(3)
Sn1–O1^{i}	2.339(2)	2.309(3)	2.282(3)
Sn1–X1	2.5421(9)	2.7211(5)	2.9838(4)
P1–O1	1.494(2)	1.492(3)	1.497(3)
C2–Sn1–C1	121.86(16)	121.3(2)	120.3(2)
C2–Sn1–C3	115.90(15)	117.1(2)	119.76(18)
C1–Sn1–C3	120.82(15)	120.59(19)	119.50(18)
C2–Sn1–O1^{i}	88.53(12)	89.32(15)	89.34(16)
C1–Sn1–O1^{i}	85.02(12)	86.48(15)	86.32(15)
C3–Sn1–O1^{i}	84.64(10)	84.60(13)	84.72(12)
C2–Sn1–X	95.11(12)	93.89(14)	93.06(14)
C1–Sn1–X	93.87(11)	93.40(13)	92.31(13)
C3–Sn1–X	92.87(9)	92.29(11)	91.23(10)
O1^{i}–Sn1–X	176.23(7)	176.30(8)	175.92(8)
O1–P1–C4	112.68(14)	112.74(19)	112.97(18)
P1–C4–C3	113.0(2)	112.9(2)	113.4(3)
C4–C3–Sn1	113.46(18)	114.0(2)	114.7(2)
P1–O1–Sn1^{ii}	173.37(16)	170.4(2)	165.40(19)
P1–C4–C3–Sn1	175.26(16)	175.3(2)	175.84(19)

Symmetry transformations: *i*; $x + 1/2, -y + 1/2, -z$. *ii*; $x - 1/2, -y + 1/2. -z$.

found at 598–597, 554–551, 516–513, 491–490, 480–478, 425–423, 304–303 and 281–280 cm^{-1}.

The values of ν_s(NCS) and ν_{as}(NCS) in (**2**: X = NCS) in KBr are 1064 and 2066 cm^{-1}, respectively.

Conclusions

As indicated in the Introduction, the structural results of the crystallisation of (**2**: X = Cl, Br or I) clearly indicate differences between the use of alcohol solvents, on one hand, and other solvents (chlorocarbon, acetone and ether), on the other. As the un-hydroxylated solvents include good as well as poor donor solvents, the effect of the alcohols cannot be linked to their donor abilities. The one property of the alcohols, which really distinguishes them from the other solvents, is their H-bonding ability. In particular, the ability of alcohols to form strong H-bonds with phosphine oxides is well documented.[11,12]

The chelate effect generally indicates that chelate complexes are preferred over alternative non-chelated complexes. However both entropy and enthalpy terms contribute to the chelate effect, and as little, if any, difference should be found in the enthalpic effects for *chelate*-(**2**) and *polymeric*-(**2**), differences in entropy terms for the different forms of **2** in different solvents must be the significant factors. It is argued that the linear chain forms of **2** are preferred over chelated forms in alcohols as a consequence of the greater extent of H-bonding between the alcohol solvents and the P–O group in the polymer-form. The oxygen atom in the molecular chelated complex is in a more sterically crowded environment than in the linear chain version of **2**. Thus the polymer form should be more readily solvated. Hence in alcohol solvents, the linear chain species should be more heavily solvated (H-bonded) and to such an extent that the solvation/entropy effects render this the preferred structure. We conclude that since the H-bonding abilities of the alcohol solvents result in the highly solvated linear chain forms of **2** being favoured, crystallisation of **2** from such solvents most readily provides the polymeric forms. In solvents less able to H-bond, the molecular chelated species are the favoured forms. It was earlier reported that (**2**: X = I) was found, by osmometry, to be monomeric in $CHCl_3$ solution.[10] It is important to point out that neither set of forms is solvated in the solid state.

It is apparent that crystallisation of (**2**: X = NCS) is unaffected by the solvent.

Experimental

Melting points were measured using a Kofler hot stage microscope and are uncorrected. NMR spectra were obtained on Bruker 250 MHz and Bruker 400 MHz instruments; IR spectra were recorded on a Nicolet Magna-IR 760 instrument. DSC experiments were conducted on a Mettler Toledo DSC 821^{e} instrument and TGA/MS on a Mettler Toledo TGA/SDTA

Table 5 Selected infrared spectral data for **2** in KBr

Compound	Recrystallisation solvent	Monomer or polymer	ν(PO)/cm^{-1}
(**2**: X = Me)			1181(vs), 1163(sh), 1120(s)
(**2**: X = Cl)	Me_2CO	monomer	1156(sh), 1139(vs), 1126(sh)
(**2**: X = I)	$CHCl_3$	monomer	1133(vs)
(**2**: X = NCS)	MeOH	monomer	1158(sh), 1133(vs)
(**2**: X = NCS)	$CHCl_3$	monomer	1158(sh), 1134(vs)
(**2**: X = Cl)	MeOH	polymer	1168(vs), 1159(sh), 1139(w), 1126(s)
(**2**: X = Br)	MeOH	polymer	1166(vs), 1159(sh), 1136(sh), 1126(s)
(**2**: X = I)	EtOH	polymer	1162(sh), 1156(vs), 1126(s)
Compound	Recrystallisation solvent	Monomer or polymer	ν/cm^{-1}
(**2**: X = Cl)	Me_2CO	monomer	555(vs), 533(s), 504(w), 497(m), 481(s), 442(m), 383(m), 334(w), 305(w), 287(w), 250(vs), 200(w), 163(m).
(**2**: X = Cl)	MeOH	polymer	598(vs), 533(vs), 534(s), 516(s), 491(s), 480(m), 443(w), 425(w), 384(w), 303(w), 280(w), 248(m), 234(s), 163(m)
(**2**: X = Br)	MeOH	polymer	598(s), 554(vs), 532(vs), 515(s), 505(w), 491(w), 480(s), 442(m), 423(w), 384(m), 335(w), 304(m), 284(w), 233(w)
(**2**: X = I)	$CHCl_3$	monomer	561(vs), 544(m), 530(s), 501(m), 492(m), 478(s), 442(s), 382(m), 338(w), 314(s), 256(w), 229(w), 196(w)
(**2**: X = I)	EtOH	polymer	597(vs), 551(s), 531(m), 513(vs), 490(s), 478(s), 420(w), 393(w), 300(w), 280(w), 193(w), 184(w).
(**2**: X = NCS)	MeOH	monomer	565(sh), 559(vs), 536(vs), 511(m), 489(vs), 476(s), 445(s), 388(m), 338(w), 318(m), 225(s), 196(w), 175(w).
(**2**: X = NCS)	$CHCl_3$	monomer	565(sh), 559(vs), 536(vs), 512(m), 489(vs), 476(s), 445(s), 388(m), 338(w), 319(m), 224(s), 196(w), 172(w).

vs = very strong, s = strong, sh = shoulder.

Table 6 Crystal data and structure refinement for molecular **2**[a]

	(**2**: X = Cl)	(**2**: X = Br)	(**2**: X = I)	(**2**: X = I)	(**2**: X = SCN)
Empirical formula	$C_{16}H_{20}ClOPSn$	$C_{16}H_{20}BrOPSn$	$C_{16}H_{20}IOPSn$	$C_{16}H_{20}IOPSn$	$C_{17}H_{20}NOPSn$
M	413.43	457.89	504.88	504.88	436.06
T/K	301(2)	301(2)	301(2)	150(2)	301(2)
Wavelength/Å	0.71073	0.71073	0.71073	0.71073	0.71073
Crystal system	Monoclinic	Monoclinic	Monoclinic	Monoclinic	Triclinic
Space group	$P2_1/a$	$P2_1/a$	$P2_1/n$	$P2_1/n$	$P\bar{1}$
a/Å	9.7708(4)	9.8150(4)	13.6367(5)	13.5071(12)	10.9789(4)
b/Å	15.1394(6)	15.2192(7)	10.3643(4)	10.2104(9)	12.3397(5)
c/Å	12.6876(5)	12.8056(6)	13.8351(6)	13.8162(10)	15.0045(6)
α/°	90	90	90	90	86.3850(10)
β/°	109.9570(10)	109.6080(10)	95.7490(10)	95.722(2)	82.3080(10)
γ/°	90	90	90	90	78.4830(10)
V/Å^{-3}	1764.10(12)	1801.93(14)	1945.55(13)	1985.9(3)	1972.52(13)
Z	4	4	4	4	4
Calculated density/Mg m^{-3}	1.577	1.688	1.724	1.769	1.468
Absorption coefficient/mm^{-1}	1.684	3.718	2.977	3.055	1.483
F(000)	824	896	968	968	872
Crystal colour	colourless	colourless	colourless	colourless	colourless
Crystal size/mm	0.44 × 0.28 × 0.24	0.30 × 0.20 × 0.20	0.40 × 0.30 × 0.30	0.10 × 0.04 × 0.02	0.42 × 0.40 × 0.29
θ range for data collection/°	1.71–24.99	1.69–24.98	2.00–25.03	2.01–27.44	1.37–25.03
Index range	$-11 \le h \le 10$ $-18 \le k \le 16$ $-14 \le l \le 15$	$-11 \le h \le 11$ $-15 \le k \le 18$ $-15 \le l \le 15$	$-16 \le h \le 16$ $-12 \le k \le 12$ $-7 \le l \le 16$	$-17 \le h \le 17$ $-12 \le k \le 13$ $-17 \le l \le 17$	$-12 \le h \le 13$ $-14 \le k \le 13$ $-17 \le l \le 17$
Reflections collected/unique	10432/3104	10722/3168	10722/3168	16105/4272	12048/6938
R(int)	0.0186	0.0241	0.0241	0.0931	0.0151
Completeness to 2θ limit (%)	99.6	99.7	94.1	93.4	99.4
Max. and min. transmission	0.862 and 0.702	0.9280 and 0.7241	0.8620 and 0.5400	0.933 and 0.811	0.9280 and 0.7932
Data/restraints/parameters	3104/0/183	3168/0/183	3434/0/183	4272/0/183	6938/0/401
Goodness-of-fit on F^2	1.030	1.032	1.031	1.014	1.014
Final R indices [$I > 2\sigma(I)$] $R1$	0.0195	0.0239	0.0293	0.0503	0.0271
$wR2$	0.0499	0.0584	0.0741	0.1067	0.0690
R indices (all data) $R1$	0.0242	0.0329	0.0372	0.1190	0.0368
$wR2$	0.0520	0.0610	0.07967	0.1366	0.0743
Largest diff. peak and hole/e Å^{-3}	0.371 and −0.287	0.821 and −0.784	0.826 and −0.817	1.708 and −0.891	0.730 and −0.466

[a] In all cases absorption correction used: semi-empirical from equivalents; refinement method: full-matrix least squares on F^2.

851[e] instrument connected to a Balzers Thermostar MS. A Hägg Guinier focussing camera, with Cu-Kα_1 radiation was used to obtain the powder patterns.

Synthesis

Compound (2: X = Me). This was obtained as reported.[10]

Compound (2: X = Cl). This was obtained by addition of a solution of HCl (12 mmol) in EtOH to a solution of (**2**: X = Me) (4.72 g, 12 mmol) in Et_2O (50 ml), by a similar method used to prepare (**1**: X = Cl).[4] After stirring for 1 h, the solution was rotary evaporated and the residue was initially recrystallised from CH_2Cl_2/petroleum ether (bp 60–80 °C).

Table 7 Crystal data and structure refinement for polymeric **2**

	(**2**: X = Cl)	(**2**: X = Br)	(**2**: X = I)
Empirical formula	$C_{16}H_{20}ClOPSn$	$C_{16}H_{20}BrOPSn$	$C_{16}H_{20}IOPSn$
M	413.43	457.89	504.88
T/K	301(2)	301(2)	301(2)
Wavelength/Å	0.71073	0.71073	0.71073
Crystal system	*P*2(1)2(1)2(1)	*P*2(1)2(1)2(1)	*P*2(1)2(1)2(1)
Space group	Orthorhombic	Orthorhombic	Orthorhombic
a/Å	10.9671(4)	10.8817(5)	10.7840(4)
b/Å	11.8140(5)	11.8135(5)	11.9471(5)
c/Å	13.7591(5)	13.9015(5)	14.2380(6)
α/°	90	90	90
β/°	90	90	90
γ/°	90	90	90
V/Å^3	1782.70(12)	1785.05(13)	1834.39(13)
Z	4	4	4
Calculated density/Mg m^{-3}	1.540	1.702	1.828
Absorption coefficient/mm^{-1}	1.666	3.749	3.157
F(000)	824	896	968
Crystal colour	colourless	colourless	colourless
Crystal size/mm	0.32 × 0.22 × 0.22	0.37 × 0.30 × 0.24	0.32 × 0.22 × 0.19
θ range for data collection/°	2.27–25.00	2.26–25.02	2.23– 25.01
Index range	$-13 \le h \le 13$ $-12 \le k \le 14$ $-16 \le l \le 15$	$-12 \le h \le 09$ $-14 \le k \le 14$ $-16 \le l \le 16$	$-12 \le h \le 12$ $-13 \le k \le 14$ $-12 \le l \le 16$
Reflections collected/unique	10689/3119	10875/3137	11013/3222
[*R*(int)]	[0.0239]	[0.0303]	[0.0263]
Completeness to 2*θ* limit (%)	99.8	99.8	99.9
Absorption correction	Semi-empirical from equivalents	Semi-empirical from equivalents	Semi-empirical from equivalents
Max. and min. transmission	0.8619 and 0.6837	0.862 and 0.594	0.86190 and 0.6127
Refinement method	Full-matrix least squares on F^2	Full-matrix least squares on F^2	Full-matrix least squares on F^2
Data/restraints/parameters	3119/0/183	3137/0/183	3222/0/183
Goodness-of-fit on F^2	0.998	0.957	1.014
Final *R* indices [$I > 2\sigma(I)$] *R*1	0.0183	0.0222	0.0185
*wR*2	0.0426	0.0465	0.0430
R indices (all data) *R*1	0.0204	0.0276	0.0202
*wR*2	0.0432	0.0478	0.0436
Absolute structure parameter	0.018(19)	0.029(9)	−0.01(2)
Largest diff. peak and hole/e Å^{-3}	0.257 and −0.208	0.424 and −0.303	0.666 and −0.339

Anal. for (**2**: X = Cl): Found: C, 46.4; H, 4.0. $C_{16}H_{20}ClOPSn$ requires: C, 46.5; H, 4.9%.

Compounds (2: X = Br, I or SCN). These were generally obtained from (**2**: X = Cl) (1.24 g, 3 mmol) by halogen exchange using a 10-fold excess of NaX (X = Br, I or SCN) in acetone (50–100 ml). After stirring the reaction mixture for 4 h at ambient temperature, the precipitate was removed and the filtrate evaporated. The residue was redissolved in $CHCl_3$, filtered, and the solution evaporated. Recrystallisations of this initial product, either from cold EtOH or $CHCl_3$, were continued until NMR/chemical analysis indicated that a pure exchange product had been isolated. Subsequent recrystallisations were from specific organic solvents. The purity of the exchange products was the prime concern rather than yields. The analytical data presented below are for samples recrystallised from EtOH and used in the structure determinations: samples recrystallised from other solvents also had acceptable analyses. Anal for (**2**: X = Br): Found: C, 42.2; H, 4.3. $C_{16}H_{20}BrOPSn$ requires C, 42.0; H, 4.4%. (**2**: X = I): Found: C, 38.3; H, 4.1. $C_{16}H_{20}IOPSn$ requires C, 38.1; H, 4.0%. (**2**: X = NCS): Found: C, 46.7; H, 4.7; N, 3.3. $C_{17}H_{20}NOPSSn$ requires C, 46.8; H, 4.6; N, 3.2%.

Compound (2: X = I). This was also obtained from (**2**: X = Me) (1.089, 3 mmol) in $CHCl_3$ (10 ml) and iodine (0.76 g, 3 mmol) in $CHCl_3$ (30 ml). Solutions of the two reagents were mixed and left stirring at 20 °C until the reaction mixture was colourless. All volatiles were removed under vacuum and the residue was recrystallised from EtOH. The compound was identical to a sample obtained by halide exchange with (**2**: X = Cl) which had been recrystallised from EtOH.

Melting points and solvents used in the final recrystallisations are given in Table 2. Solution NMR spectral data are listed in Table 1. Selected infrared data are listed in Table 5.

Crystallography

Intensity data for (**2**: X = Cl, Br, I and SCN) at ambient temperature (301 K) were obtained with a Bruker SMART 1000 CCD diffractometer. SMART software was used for data collection and SAINT software for cell refinement and data reduction.[13] Absorption correction by the multi-scan technique was made using SADABS.[14] SHELXS-86 was used to solve the structure by the heavy atom technique.[15] The initial solution was expanded and refined with SHELXL-97.[16]

Intensity data for (**2**: X = I) at 150 K were collected by the EPSRC service, based at the University of Southampton, with an Enraf Nonius KappaCCD diffractometer. The programs DENZO[17] and COLLECT[18] were used for data collection, cell refinement and data reduction. SORTAV was used to apply absorption correction by the multi-scan technique.[19] The structure was solved by the heavy atom method with SHELXS-86[15] and refined with SHELXL-97.[16] All non-H atoms were refined anisotropically and H atoms were placed in calculated positions and refined with a riding model. Crystal data and structure refinement details for molecular and polymeric **2** are summarised in Tables 6 and Table 7.

CCDC reference numbers 167268–167275.

See http://www.rsc.org/suppdata/dt/b1/b103107b/ for crystallographic data in CIF or other electronic format.

Acknowledgements

We acknowledge the use of the National Data Collection

Service of the EPSRC at the University of Southampton and the expert assistance of the staff there. We also thank Mr B. J. A. Paterson for obtaining the thermal analyses data and Mr J. Marr for the powder diffraction work.

References

1 J. T. B. H. Jastrzebski and G. van Koten, *Adv. Organomet. Chem.*, 1993, **35**, 241.

2 *e.g.* A. R. Forrester, S. J. Garden, R. A. Howie and J. L. Wardell, *J. Chem. Soc., Dalton Trans.*, 1992, 2615; A. R. Forrester, R. A. Howie, J.-N. Ross, J. N. Low and J. L. Wardell, *Main Group Metal Chem.*, 1991, **14**, 293; C. C. C. Chibesakunda, P. J. Cox, H. Rufino and J. L. Wardell, *Acta Crystallogr., Sect. C*, 1998, **54**, 893; H. C. Dai, Q. H. Yung, X. H. Wang, S. M. Yue, H. de Pan and X. Chen., *Polyhedron*, 1998, **17**, 2503; F. Fu, H. Li, D. Zhu, Q. Fang, H. Pan, E. R. T. Tiekink, F. Kayser, M. Biesemans, I. Verbruggen, R. Willem and M. Gielen, *J. Organomet. Chem.*, 1995, **490**, 163; F. Kayser, M. Biesemans, A. Delmotte, I. Verbruggen, I. De Borger, M. Gielen, R. Willem and E. R. T. Tiekink, *Organometallics*, 1994, **13**, 4026.

3 U. Kolb, M. Drager and B. Jousseaume, *Organometallics*, 1991, **10**, 2737.

4 (*a*) H. Weichmann, C. Mugge, A. Grand and J. B. Robert, *J. Organomet. Chem.*, 1982, **238**, 343; (*b*) H. Preut, B. Godry and T. N. Mitchell, *Acta Crystallogr., Sect. C*, 1992, **48**, 1894.

5 P. J. Cox, S. M. S. V. Doidge-Harrison, R. A. Howie, I. W. Nowell, O. J. Taylor and J. L. Wardell, *J. Chem. Soc., Perkin Trans. 2*, 1989, 2017.

6 P. J. Cox, S. J. Garden, R. A. Howie, O. A. Melvin and J. L. Wardell, *J. Organomet. Chem.*, 1996, **516**, 213.

7 M. Biesemans, R. Willem, S. Darmoun, P. Geerlings, E. R. T. Tiekink, M. Lahcini and B. Jousseaume, *Organometallics*, 1998, **17**, 90.

8 M. Biesemans, R. Willem, S. Darmoun, P. Geerlingsa, M. Lahcini, P. Jaumier and B. Jousseaume, *Organometallics*, 1996, **15**, 2237; P. Jaumier, B. Jousseaume, E. R. T. Tiekink, M. Biesemans and R. Willem, *Organometallics*, 1997, **16**, 5124.

9 J. J. R. F. da Silva, *J. Chem. Educ.*, 1983, **60**, 390; W. P. Jencks, *Proc. Natl. Acad. Sci. USA*, 1981, **78**, 4046.

10 (*a*) T. N. Mitchell and B. Godry, *J. Organomet. Chem.*, 1995, **490**, 45; (*b*) H. Weichmann, G. Quell and A. Tzschach, *Z. Anorg. Allg. Chem.*, 1980, **462**, 7.

11 M. J. Kamlet, J.-M. Abboud, M. H. Abraham and R. W. Taft, *J. Org. Chem.*, 1983, **48**, 2877; M. J. Kamlet, J.-M. Abboud and R. W. Taft, *Prog. Phys. Org. Chem.*, 1981, **13**, 485.

12 T. Gramstad, S. Husebye and K. Maartmann-Moe, *Acta Chem. Scand. Ser. B*, 1986, **40**, 26; M. Akazome, S. Suzuki, Y. Shimizu, K. Henmi and K. Ogura, *J. Org. Chem.*, 2001, **65**, 6917; J. C. Harge, H. E. Elabdalloaui and P. Rubini, *Magn. Reson. Chem.*, 1993, **31**, 752; M. Dargatz, H. Hartung, E. Kleinpeter, B. Rensch, D. Schollmeyer and H. Weichmann, *J. Organomet. Chem.*, 1989, **361**, 43.

13 SMART and SAINT software for area-detector diffractometers, Bruker Analytical X-ray Systems, Madison, Wisconsin, USA, 1999.

14 G. M. Sheldrick, SADABS, Program for scaling and correction of area detector data, University of Göttingen, Germany, 1997.

15 G. M. Sheldrick, *Acta Crystallogr., Sect. A*, 1990, **46**, 467.

16 G. M. Sheldrick, SHELX-97, Program for crystal structure refinement, University of Göttingen, Germany, 1997.

17 Z. Otwinowski and W. Minor, *Methods in Enzymology, Vol. 276: Macromolecular Crystallography, Part A*, ed. C. W. Cater and R. M. Sweet, Academic Press, New York and London, 1997, pp. 307–326.

18 R. Hooft, COLLECT, Nonius BV, Delft, The Netherlands, 1998.

19 R. H. Blessing, *Acta Chem. Scand. Ser. A*, 1995, **51**, 33; R. H. Blessing, *J. Appl. Crystallogr.*, 1997, **30**, 421.